Drug Design, Development and Therapy

Dovepress
open access to scientific and medical research

Open Access Full Text Article

ORIGINAL RESEARCH

Dexmedetomidine's Effects on the Livers and Kidneys of Rats with Pancreatic Ischemia-Reperfusion Injury

Hasan Bostancı[1], Selin Erel[2], Ayşegül Küçük[3], Gülay Kip[2], Şaban Cem Sezen[4], Seda Gokgoz[5], Muharrem Atlı[4], Feyza Aktepe[2], Kursat Dikmen[1], Mustafa Arslan[2,6,7], Mustafa Kavutçu[5]

[1]Gazi University Faculty of Medicine, Department of General Surgery, Ankara, Turkey; [2]Gazi University Faculty of Medicine Department of Anesthesiology and Reanimation, Ankara, Turkey; [3]Kutahya Health Sciences University Faculty of Medicine, Department of Physiology, Kutahya, Turkey; [4]Kırıkkale University Faculty of Medicine, Department of Histology and Embryology, Kırıkkale, Turkey; [5]Gazi University Faculty of Medicine, Department of Medical Biochemistry, Ankara, Turkey; [6]Gazi University, Life Sciences Application and Research Center, Ankara, Turkey; [7]Gazi University, Laboratory Animal Breeding and Experimental Research Center (GUDAM), Ankara, Turkey

Correspondence: Ayşegül Küçük, Kutahya Health Sciences University, Medical Faculty, Department of Physiology, Kutahya, Turkey, Tel +90 532 675 77 05, Email aysegul.kucuk@gmail.com

Objective: Pancreatic surgeries inherently cause ischemia-reperfusion (IR) injury, affecting not only the pancreas but also distant organs. This study was conducted to explore the potential use of dexmedetomidine, a sedative with antiapoptotic, anti-inflammatory, and antioxidant properties, in mitigating the impacts of pancreatic IR on kidney and liver tissues.

Methods: A total of 24 rats were randomly divided into four groups: control (C), dexmedetomidine (D), ischemia reperfusion (IR), and dexmedetomidine ischemia reperfusion (D-IR). Pancreatic ischemia was induced in the IR and D-IR groups. Dexmedetomidine was administered intraperitoneally to the D and D-IR groups. Liver and kidney tissue samples were subjected to microscopic examinations after hematoxylin and eosin staining. The levels of thiobarbituric acid reactive substances (TBARS), aryllesterase (AES), catalase (CAT), and glutathione S-transferase (GST) enzyme activity were assessed in liver and kidney tissues. The serum levels of aspartate aminotransferase (AST), alanine aminotransferase (ALT), blood urea nitrogen (BUN), and creatinine were measured.

Results: A comparison of the groups revealed that the IR group exhibited significantly elevated TBARS ($p < 0.0001$), AES ($p = 0.004$), and CAT enzyme activity ($p < 0.0001$) levels in the liver and kidney compared to groups C and D. Group D-IR demonstrated notably reduced histopathological damage ($p < 0.05$) and low TBARS ($p < 0.0001$), AES ($p = 0.004$), and CAT enzyme activity ($p < 0.0001$) in the liver and kidney as well as low AST and ALT activity levels ($p < 0.0001$) in the serum compared to the IR group.

Conclusion: The preemptive administration of dexmedetomidine before pancreatic IR provides significant protection to kidney and liver tissues, as evidenced by the histopathological and biochemical parameters in this study. The findings underscored the potential therapeutic role of dexmedetomidine in mitigating the multiorgan damage associated with pancreatic surgeries.

Keywords: pancreas, ischemia-reperfusion, dexmedetomidine, liver, kidney

Introduction

The mechanism underlying the damage caused by ischemia-reperfusion (IR) injury in various organs has previously been explored. It is widely acknowledged that the harm inflicted on tissues due to a lack of blood flow becomes more noticeable and more severe when blood and oxygen are reintroduced into previously ischemic tissues during reperfusion. The occurrence of ischemia and subsequent reperfusion leads to the disruption of small blood vessels in the pancreas, which is a key factor in the development of acute pancreatitis. Pancreatic IR is caused by reduced blood flow in the abdomen due to posttraumatic bleeding, septic conditions, cardiovascular disorders, clot formation due to the blockage of blood vessels, and surgical procedures such as aortic arch surgery, which involves the redirection of blood flow or clamping of blood vessels.[1,2] Notably, pancreatic IR injury also arises in cases of pancreatic surgery, such as transplantation and pancreaticoduodenectomy.[2]

The kidneys and liver are particularly susceptible to ischemia. Recent studies have shed light on the occurrence of acute kidney injury (AKI) following major abdominal surgery, emphasizing its potentially fatal consequences.[3–6] Within

Received: 23 September 2023
Accepted: 13 May 2024
Published: 27 May 2024

the realm of pancreatic surgeries, graft pancreatitis is associated with a heightened risk of severe IR injury, which occurs in up to 25% of cases in the postoperative period. This complication can, in turn, significantly increase the risk of pancreas IR, leading to subsequent kidney and liver injuries.[1,7–9] Therefore, developing effective treatments and protective mechanisms is of utmost importance.

Dexmedetomidine, which is characterized by its strong selectivity for the alpha-2 adrenergic receptor, has sedative, pain-relieving, and sympathetic nervous system suppressive effects.[10,11] Numerous investigations have highlighted the anti-inflammatory effects of dexmedetomidine in response to infection as well as its ability to inhibit inflammatory factors in cases of shock and ischemia-reperfusion injury.[12–15] Furthermore, dexmedetomidine exerts protective effects on various organs, including the brain,[12] heart,[16] lungs,[14] intestines,[17] and kidneys.[13]

While the literature emphasizes dexmedetomidine's protective effects on acute pancreatitis induced by pharmacological agents, such as sodium taurocholate and caerulein,[18,19] there is a gap in research regarding distant organ damage resulting from surgical pancreatic IR. Therefore, this study was conducted to assess the cytoprotective properties of dexmedetomidine when administered therapeutically, focusing on liver and kidney cell injuries and dysfunction following pancreatic IR injury.

Materials and Methods

Animals and Experimental Protocol

This study was conducted with the consent of the Experimental Animal Ethics Committee of Gazi University (G.Ü.ET-23.076). All procedures were performed in accordance with the accepted standards of the Guide for the Care and Use of Laboratory Animals and the ARRIVE guidelines for animal welfare.

A total of 24 male Wistar albino male rats, aged five months and weighing 200–225 g, were used in this study. The rats were kept at a temperature of 20–21°C in cycles of 12 h of daylight and 12 h of darkness and had free access to food until two hours before an anesthetic procedure. The animals were randomly separated into four groups—control (group C), dexmedetomidine (group D), ischemia reperfusion (group IR), and dexmedetomidine ischemia reperfusion (group D-IR)—each containing six rats (n = 6). Prior to the experiment, all rats were anesthetized with 50 mg/kg intramuscular ketamine (Ketalar®; 1 mL = 50 mg; Pfizer, Istanbul, Turkey) and 10 mg/kg xylazine hydrochloride (Alfazyne® 2%; Ege Vet, Turkey). To avoid hypovolemia, 3 mL/kg intraperitoneal 0.9% NaCl was administered hourly to all groups. During the ischemia-reperfusion period, the abdomens were covered with moistened, sterile pads.

Control group (Group C): Midline laparotomy was performed without any additional surgical intervention. After 3 h of follow-up, the liver and kidney tissues were excised after the rats were sacrificed under anesthesia.

Dexmedetomidine group (Group D): Midline laparotomy was performed without any additional surgical intervention. 100 µg/kg dexmedetomidine (Sedodamid 100 µg/2 mL, Koçak Farma®, Turkey)[20] was administered intraperitoneally 30 min before laparotomy. Laparotomy was the sole surgical procedure conducted, without IR intervention. Three hours after the procedure, the liver and kidney tissues were excised after the rats were sacrificed under anesthesia.

Ischemia reperfusion group (Group IR): A pancreatic IR model was established as described in the literature.[21] A midline laparotomy was performed on the rats; the gastric breves were dissected and ligated, and the omentum majus was separated from the greater curvature of the stomach. For complete ischemia of the pancreas, the gastroduodenal, left gastric, splenic, and caudal pancreaticoduodenal arteries were isolated and clamped using an atraumatic microvascular clamp. After 60 min of ischemia and 120 min of reperfusion, the liver and kidney tissues of the rats were excised under anesthesia after euthanasia.[22]

Dexmedetomidine ischemia reperfusion (Group D-IR): Dexmedetomidine (Sedodamid 100 µg/2 mL, Koçak Farma®, Turkey) (100 µg/kg)[20] was intraperitoneally administered 30 min after midline laparotomy was performed. The gastric breves were dissected and ligated, and the omentum majus was separated from the greater curvature of the stomach. The gastroduodenal, left gastric, splenic, and caudal pancreaticoduodenal arteries were isolated and clamped. After 60 min of ischemia and 120 min of reperfusion, the liver and kidney tissues of the rats were excised after sacrifice under anesthesia.

Following reperfusion, blood samples were collected from the abdominal aortas of the rats. Subsequently, the rats were anesthetized via intraperitoneal injections of ketamine (100 mg/kg) and xylazine (10 mg/kg) and sacrificed by

collecting abdominal aorta blood. At the end of the experiment, liver and kidney tissue samples were collected from all the rats for biochemical and histopathological evaluations.

After their heartbeats and respiration ceased, the rats were monitored for 2 min to confirm death.

Biochemical Analysis

The blood samples were collected in tubes. After centrifugation, aspartate aminotransferase (AST), alanine amino transaminase (ALT), and gamma glutamyl transferase (GGT) activity levels and blood urea nitrogen (BUN) and creatinine levels were measured using an Abbott Architect c16000 auto analyzer.

Aryllesterase (AES), catalase (CAT) and glutathione S-transferase (GST) activity levels and thiobarbituric acid reactive substance (TBARS) levels were measured in the liver and kidney tissue samples. The liver and kidney tissues were initially rinsed with cold 0.154 M NaCl solution to remove any blood contamination and then homogenized using a homogenizer (Heidolph Instruments GMBH & CO KGDiax 900, Germany) at 1000 rpm for approximately 3 min. The samples were centrifuged at 10,000 x g for 10 min at 4°C, and the resulting upper clear layer was collected for further analysis.

To quantify the TBARS (as malondialdehyde) levels, a thiobarbituric acid (TBA) reactive substance assay was utilized, as outlined in the literature.[23] This method involves a reaction with TBA at a temperature of 85–90°C to determine the malondialdehyde concentration. Malondialdehyde, and similar compounds, reacts with TBA to generate a pink pigment, and its highest absorption is exhibited at 532 nm. Generally, to ensure protein precipitation, a room-temperature sample is mixed with cold 20% (wt/vol) trichloroacetic acid. The precipitate is then centrifuged for 10 min at 3000 rpm and room temperature to form a pellet. A portion of the supernatant is subsequently combined with an equal volume of 0.6% (wt/vol) TBA and placed in a boiling water bath for 30 min. After cooling, the absorbance of both the sample and a blank is measured at 532 nm.

Catalase (CAT) activity was measured based on whether a decrease in absorbance was caused by the consumption of hydrogen peroxide (H_2O_2) at 240 nm.[24] Further, GST activity was determined based on the measurement of absorbance increase at 340 nm due to a reduction of dinitrophenyl glutathione (DNPG), as described by Habig et al.[25] Activity measurements were performed using the ε value of the DNPG complex.

The protein amounts of the samples were determined using the Lowry method, with bovine serum albumin used as the standard protein.[26] The results were expressed as IU/mg protein for enzymes and nmol/mg protein for TBARS.

Histopathological Analysis

Histopathological assessments were performed in the Department of Histology at Kirikkale University. The tissues were fixed in 10% formalin for 48 h at room temperature. After fixation, the specimens were embedded in paraffin and subjected to routine tissue processing. Tissue sections 4 µm thick were sliced from the paraffin blocks using a microtome (Leica RM2245, Germany) and stained with hematoxylin and eosin for histopathological evaluations.

Examination of prepared specimens: Tissue sections were prepared of each group. The sections were scanned from end to end, and 1–2 images were taken from appropriate areas. Each field of view was scanned once.

The tissue sections were examined under a light microscope (Leica DM 4000 B, Germany) connected to a computer. Photographs of the samples were taken using Leica LAS V4.9. Hematoxylin and eosin-stained tissue sections were examined at 200× and 400× magnifications.

Liver

Each sample was examined for hydropic degeneration, sinusoidal dilatation, pycnotic nuclei, necrosis, and mononuclear cellular infiltration in the parenchyma. The semiquantitative evaluation technique used by Abdel-Wahhab et al[27] for histological testing was applied to interpret the structural changes in the hepatic tissues of the control and treatment groups, with a negative point (0) representing no structural changes, one positive point (1, +) indicating mild changes, two positive points (2, ++) representing medium structural changes, and three positive points (3, +++) indicating severe structural changes.[28]

Renal

Renal injury was evaluated by assessing glomerular vacuolization (GV), tubular dilation (TD), vascular vacuolization and hypertrophy (VVH), tubular cell degeneration and necrosis (TCDN), Bowman space dilation (BSD), tubular hyaline cylinders (THC), lymphocyte infiltration (LI), and tubular cell shedding (TCS).[29] Renal injuries were scored as follows: 0, no change; +1, minimal change; +2, medium; and +3, severe.[20]

Statistical Analysis

Statistical analysis was performed using the Statistical Package for the Social Sciences (SPSS, Chicago, IL, USA) version 26.0. The Shapiro–Wilk test and Q–Q plot test were used to assess the data distribution. The results were analyzed using the Kruskal–Wallis test, followed by Dunn's test or one-way ANOVA and Tukey's test. The results were expressed as mean ± standard deviation (SD) and median (interquartile range [IQR]) values. Statistical significance was set at $p < 0.05$.

Results

Liver Tissue Histopathological Results

Histopathological examinations of the liver tissues revealed significant variations between the groups in terms of hydropic degeneration, sinusoidal dilation, pyknotic nuclei, and necrosis ($p = 0.014$, $p = 0.009$, $p = 0.032$, and $p = 0.007$, respectively).

Hydropic degeneration was more common in the IR group than in the control and D-IR groups ($p = 0.001$ and $p = 0.003$, respectively). A notable decrease in hydropic degeneration was seen in the D-IR group compared to the IR group ($p = 0.034$) (Table 1 and Figures 1–4).

Similarly, sinusoidal dilation was more prominent in the IR group than in the control and D groups ($p < 0.0001$ and $p = 0.002$, respectively). However, the occurrence of sinusoidal dilatation did not differ between the D-IR and IR groups ($p = 0.051$) (Table 1 and Figures 1–4).

Pycnotic nuclei were more prevalent in the IR group than in the control and D groups ($p = 0.003$ and $p = 0.010$, respectively). A notable reduction in pycnotic nuclei instances was observed in the D-IR group compared to the IR group ($p = 0.034$) (Table 1 and Figures 1–4). Necrosis exhibited a similar pattern, being more frequent in the IR group than in the control and D groups ($p < 0.0001$ and $p = 0.001$, respectively). Further, the D-IR group displayed a significant decrease in necrosis instances compared to the IR group ($p = 0.009$) (Table 1 and Figures 1–4). Parenchymal mononuclear cell infiltration was similar across all groups (Table 1 and Figures 1–4).

Kidney Tissue Histopathological Results

Significant differences between the groups were observed in terms of GV ($p = 0.014$), TD ($p = 0.032$), VVH ($p = 0.033$), TCDN ($p = 0.021$), BSD ($p = 0.070$), THC ($p = 0.032$), LI ($p = 0.025$), and TCS ($p = 0.014$). The IR group exhibited

Table 1 Histopathological Data of Hepatic Tissue (Median [IQR])

	Group C (n = 6)	Group D (n = 6)	Group IR (n = 6)	Group D-IR (n = 6)	p**
Hydropic degeneration	0.00 (0.00–1.00)	0.50 (0.00–1.00)*	1.50 (1.00–2.00)*,&	1.00 (0.75–1.00)+	0.014
Sinusoidal dilation	0.00 (0.00–1.00)	0.50 (0.00–1.00)	2.00 (1.00–2.00)*,&	1.00 (0.75–1.00)	0.009
Pycnotic nuclei	0.50 (0.00–1.00)	0.50 (0.00–1.00)	1.50 (1.00–2.00)*,&	1.00 (0.75–1.00)+	0.032
Necrosis	0.00 (0.00–0.25)	0.00 (0.00–1.00)	1.50 (1.00–2.00)*,&	1.00 (0.00–1.00)+	0.007
Parenchymal mononuclear cell infiltration	0.50 (0.00–1.00)	0.50 (0.00–1.00)	1.00 (1.00–1.25)	1.00 (1.00–1.25)	0.174

Notes: p** Significance level obtained with the Kruskal–Wallis test, $p < 0.05$. *$p < 0.05$: Compared to Group C. &$p < 0.05$: Compared to Group D. +$p < 0.05$: Compared to Group IR.
Abbreviation: n, Number of rats.

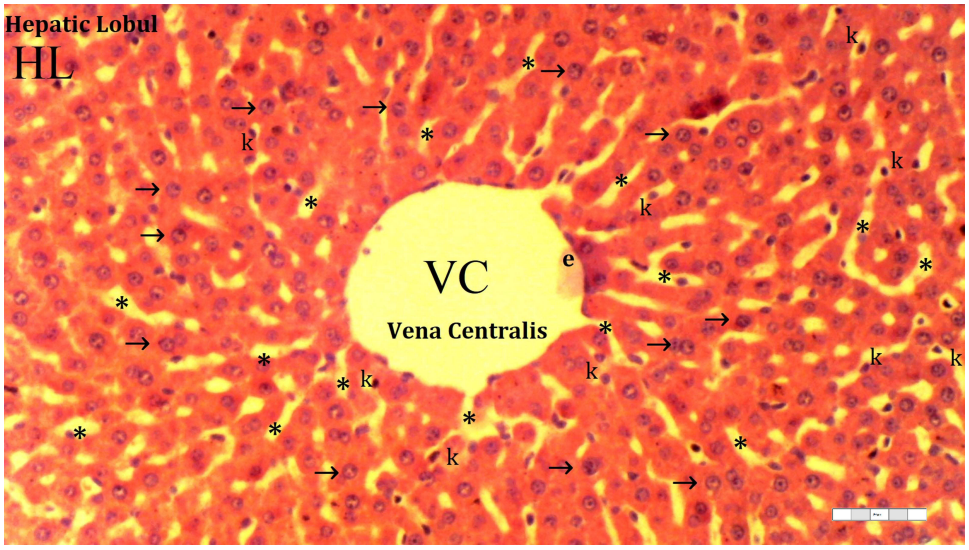

Figure 1 Representative light microscopy of hepatic tissue from the control group. Normal liver tissue.
Abbreviations: HL, hepatic lobule; VC, vena centralis; k, Kupffer cell hyperplasia; *, sinusoidal dilatation; ↓↓, infiltration; →, hepatocyte.

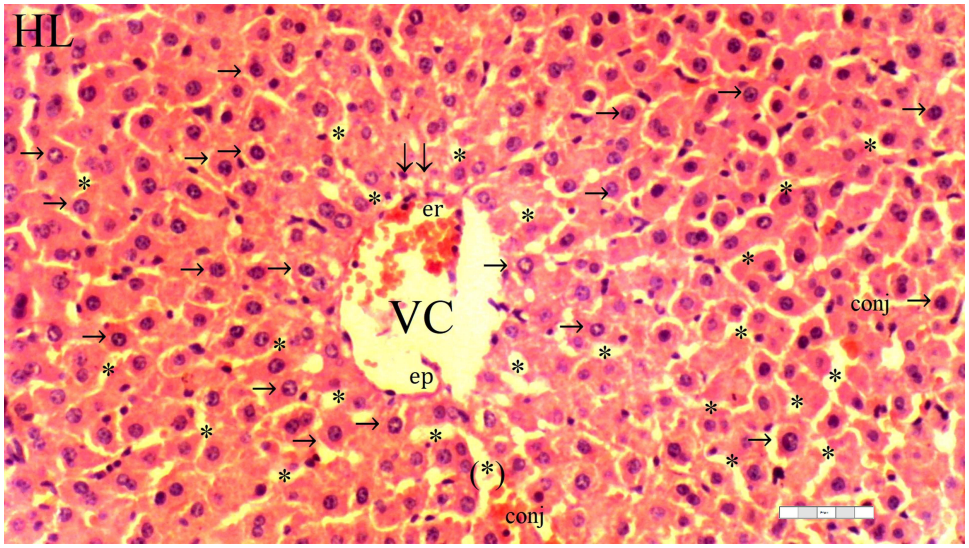

Figure 2 Representative light microscopy of hepatic tissue from the dexmedetomidine group.
Abbreviations: HL, hepatic lobule; VC, vena centralis; er, erythrocyte; ep, epitelyum; conj, congestion; *, sinusoidal dilatation; ↓↓, infiltration; →, hepatocyte.

a higher occurrence of GV than the control and D groups (p = 0.001 and p = 0.003, respectively). Moreover, GV was markedly reduced in the D-IR subgroup compared to the IR group (p = 0.034) (Table 2 and Figures 5–8).

The IR group displayed higher TD than the control and D groups (p = 0.003 and p = 0.010, respectively). The D-IR group exhibited lower TD than the IR group (p = 0.034), as summarized in Table 2 and Figures 5–8.

VVH was more frequent in the IR group than in the control and D groups (p = 0.006 and p = 0.006, respectively) (Table 2 and Figures 5–8).

The IR group exhibited higher TCDN than the control and D groups (p = 0.001 and p = 0.004, respectively). The D-IR subgroup displayed significantly lower TCDN than the IR group (p = 0.013) (Table 2 and Figures 5–8).

BSD was similar across the groups (p = 0.070) (Table 2 and Figures 5–8).

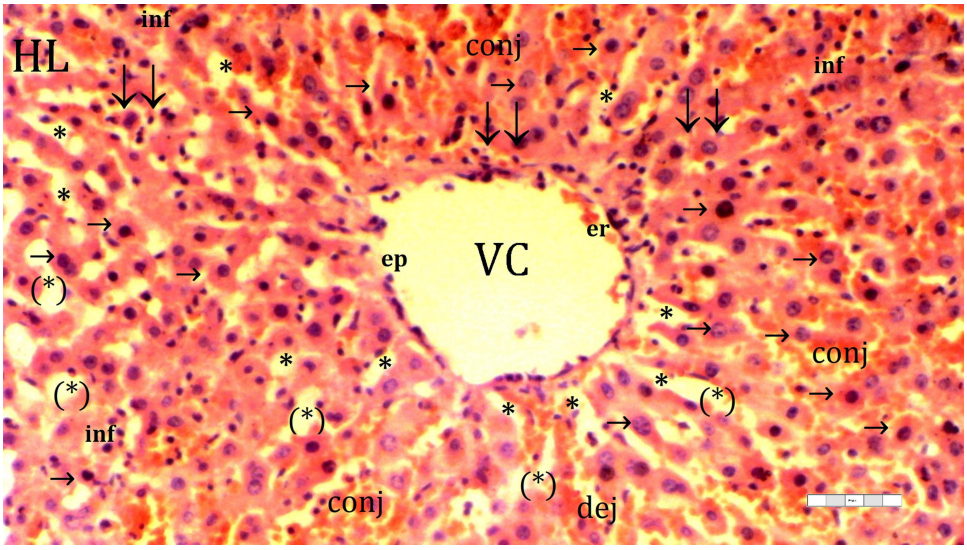

Figure 3 Representative light microscopy of hepatic tissue from the ischemia-reperfusion group.
Abbreviations: HL, hepatic lobules; VC, vena centralis; er, erythrocyte; ep, epitelyum; conj, congestion; *, sinusoidal dilatation; ↓↓, infiltration; inf, inflammation; →, hepatocyte; (*), necrotic and apoptotic hepatocyte.

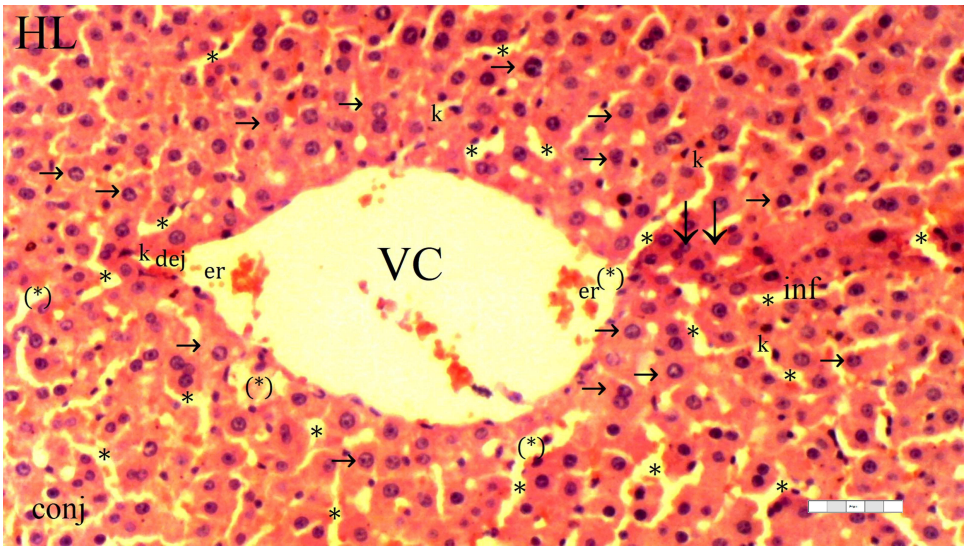

Figure 4 Representative light microscopy of hepatic tissue from dexmedetomidine ischemia-reperfusion group.
Abbreviations: HL, hepatic lobule; VC, vena centralis; er, erythrocyte; conj: congestion; *, sinusoidal dilatation; inf, inflammation; →, hepatocyte; k, Kupffer cell hyperplasia; (*), necrotic and apoptotic hepatocyte.

The IR group demonstrated a higher occurrence of THC than the control and D groups (p = 0.003 and p = 0.010, respectively). Furthermore, the D-IR subgroup displayed significantly diminished THC occurrences compared to the IR group (p = 0.034), as presented in Table 2 and Figures 5–8.

LI was more prevalent in the IR group than in the control and D groups (p = 0.003 and p = 0.003, respectively). A significant decrease in LI was observed in the D-IR group compared to the IR group (p = 0.037). Similarly, TCS exhibited a higher occurrence in the IR group than in the control and D groups (p = 0.003 and p = 0.003, respectively), and the D-IR group exhibited significantly reduced TCS compared to the IR group (p = 0.037) (Table 2 and Figures 5–8).

Table 2 Histopathological Data of the Kidney Tissue (Median [IQR])

	Group C (n = 6)	Group D (n = 6)	Group IR (n = 6)	Group D-IR (n= 6)	p**
Glomerular vacuolization (GV)	0.00 (0.00–100)	0.50 (0.00–1.00)	1.50 (1.00–2.00)*,&	1.00 (0.75–1.00)+	0.014
Tubular dilatation (TD)	0.50 (0.00–1.00)	1.00 (0.00–1.00)	1.50 (1.00–2.00)*,&	1.00 (0.75–1.00)+	0.032
Vascular vacuolization and hypertrophy (VVH)	0.50 (0.00–1.00)	0.50 (0.00–1.00)	1.50 (1.00–2.00)*,&	1.00 (0.75–1.00)	0.033
Tubular cell degeneration and necrosis (TCDN)	0.00 (0.00–1.00)	0.50 (0.00–1.00)	1.50 (1.00–2.00)*,&	1.00 (0.00–1.00)+	0.021
Bowman space dilatation (BSD)	0.50 (0.00–1.00)	0.50 (0.00–1.00)	1.50 (1.00–2.00)	1.00 (0.00–1.00)	0.070
Tubular hyaline cylinders (THC)	0.50 (0.00–1.00)	0.50 (0.00–1.00)	1.50 (1.00–2.00)*,&	1.00 (0.75–1.00)+	0.032
Lymphocyte infiltration (LI)	0.50 (0.00–1.00)	0.50 (0.00–1.00)	1.50 (1.00–2.00)*,&	1.00 (0.75–1.00)+	0.025
Tubular cell shedding (TCS)	0.00 (0.00–1.00)	0.00 (0.00–1.00)	1.50 (1.00–2.00)*,&	1.00 (0.00–1.00)+	0.014

Notes: p** Significance level obtained with the Kruskal–Wallis test, $p < 0.05$. *$p < 0.05$: Compared to group C. &$p < 0.05$: Compared to group D. +$p < 0.05$: Compared to group IR.
Abbreviation: n, Number of rats.

Liver Tissue Biochemical Results

The TBARS levels significantly differed between the groups ($p < 0.0001$). The TBARS levels were higher in the IR group than in the C and D groups ($p < 0.0001$ for both). Moreover, significantly reduced TBARS levels were found in the D-IR group compared to the IR group ($p < 0.0001$) (Table 3).

CAT enzyme activity in the liver tissues significantly differed between the groups ($p < 0.0001$). The IR group showed higher CAT enzyme activity than the C and D groups (all $p < 0.0001$). In contrast, the D-IR group exhibited lower CAT activity levels than the IR group ($p < 0.0001$), as outlined in Table 3.

Liver AES enzyme activity also significantly differed between the groups ($p = 0.004$). AES enzyme activity was higher in the IR group than in the C and D groups ($p = 0.001$ and $p = 0.002$, respectively). Conversely, the D-IR group displayed reduced AES enzyme activity compared to the IR group ($p = 0.017$) (Table 3).

Regarding GST activity in the liver tissues, no significant differences were observed between the groups ($p = 0.138$) (Table 3).

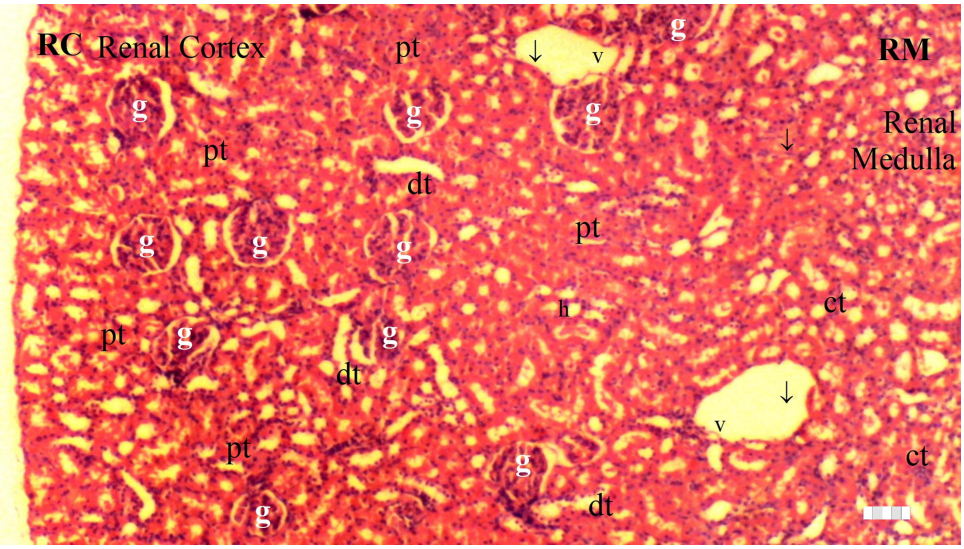

Figure 5 Representative light microscopy of kidney tissue from the control group. Normal kidney tissue.
Abbreviations: RM, renal medulla; RC, renal cortex; g, glomerulus; dt, distal tubule; pt, proximal tubule; ↓, dilate tubule; v, vacuolization.

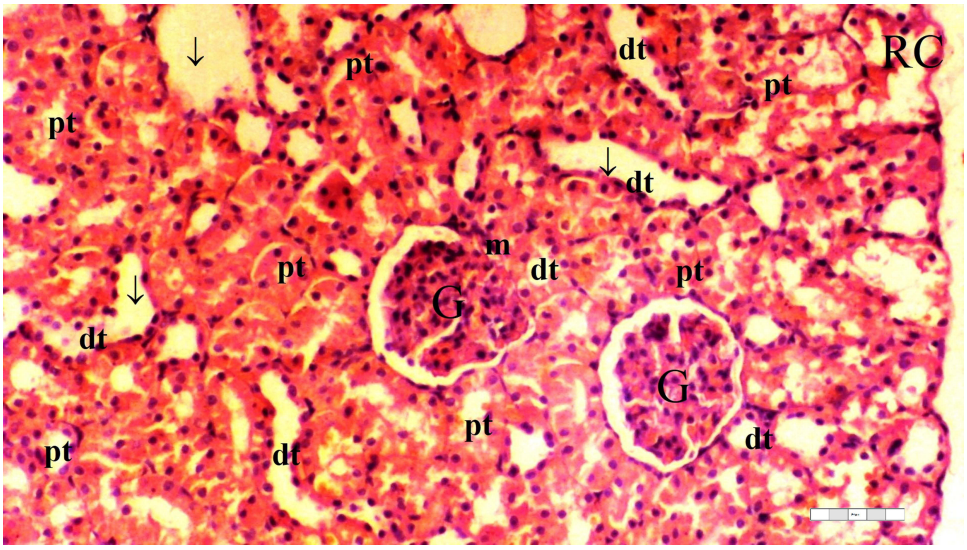

Figure 6 Representative light microscopy of kidney tissue from the dexmedetomidine group.
Abbreviations: RC, renal cortex; g, glomerulus; dt, distal tubule; pt, proximal tubule; ↓, dilate tubule; m, macula densa.

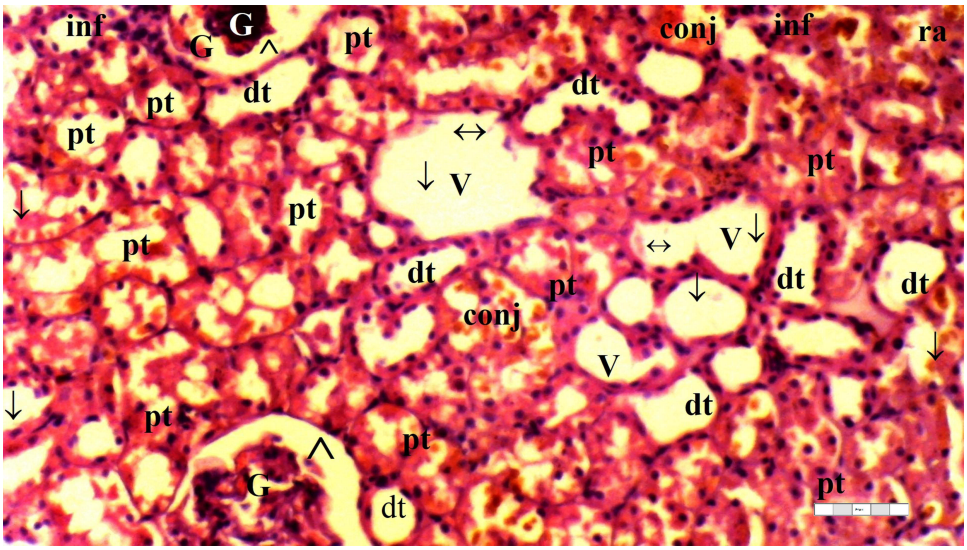

Figure 7 Representative light microscopy of kidney tissue from ischemia/reperfusion group.
Abbreviations: g, glomerulus; dt, distal tubule; pt, proximal tubule; ↓, dilate tubule; v, vacuolization; ^, Bowman space; inf, inflammation; conj, congestion.

Kidney Tissue Biochemical Results

A comparison of the kidney tissue TBARS levels revealed significant differences between the groups ($p < 0.0001$). The IR group displayed higher TBARS levels than the C and D groups ($p < 0.0001$ for both). Similarly, the D-IR group exhibited lower TBARS levels than the IR group ($p < 0.0001$) (Table 4).

CAT enzyme activity in the kidney tissues significantly differed between the groups ($p < 0.0001$). The IR group demonstrated higher CAT enzyme activity than the C and D groups (all $p < 0.0001$). In contrast, the D-IR group displayed lower CAT activity than the IR group ($p < 0.0001$) (Table 4).

The groups also had significant differences in their AES enzyme activity levels ($p < 0.0001$). AES enzyme activity was higher in the IR group than in the C and D groups (all $p < 0.0001$), whereas the D-IR group displayed reduced AES enzyme activity compared to the IR group ($p < 0.0001$) (Table 4).

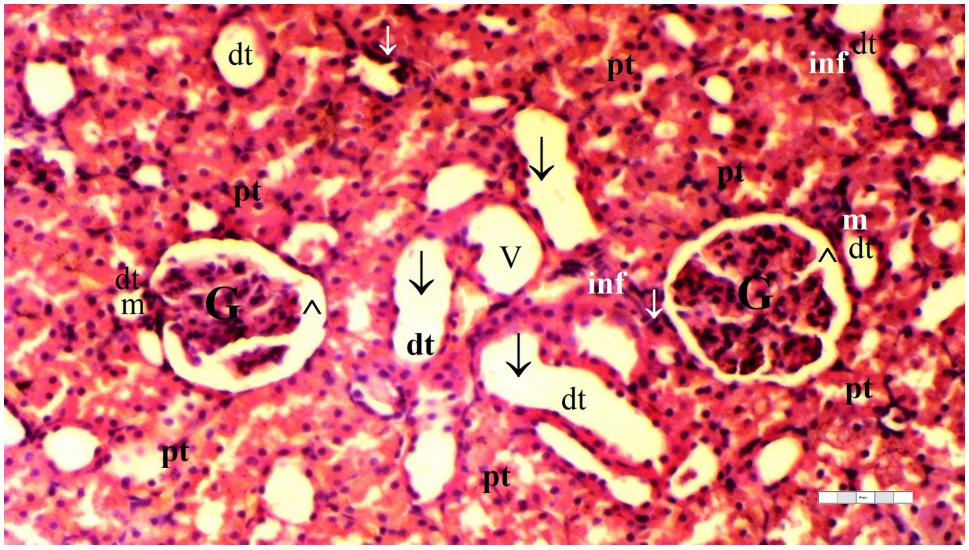

Figure 8 Representative light microscopy of kidney tissue from the dexmedetomidine ischemia-reperfusion group.
Abbreviations: g, glomerulus; dt, distal tubule; pt, proximal tubule; ↓, dilate tubule; v, vacuolization; ∧, Bowman space; inf, inflammation; m, macula densa.

Regarding GST enzyme activity in the kidney tissues, no significant differences were observed between the groups ($p = 0.810$) (Table 4).

Serum Biochemical Results

Serum AST levels significantly differed between the groups ($p < 0.0001$). AST activity was higher in the IR and D-IR groups than in the C and D groups ($p < 0.0001$ for all). However, the D-IR group displayed lower AST activity than the IR group ($p < 0.0001$) (Table 5).

Table 3 Antioxidant Enzyme Activities and Oxidant (TBARS) Levels (Mean ± SD) in Liver Tissue

	Group C (n = 6)	Group D (n = 6)	Group IR (n = 6)	Group D-IR (n = 6)	p**
TBARS (nmol/mg protein)	8.66 ± 2.00	7.23 ± 0.59	19.28 ± 2.51*,&	9.23 ± 0.83*+	< 0.0001
AES (IU/mg protein)	0.41 ± 0.13	0.47 ± 0.13	0.92± 0.31*,&	0.58 ± 0.22+	0.004
GST (IU/mg protein)	1.56 ± 0.32	1.55 ± 0.21	1.82 ± 0.17	1.75 ± 0.18	0.138
CAT (IU/mg protein)	28.28 ± 10.32	23.86 ± 10.16	81.40 ± 14.99*,&	31.28 ± 13.92+	< 0.0001

Notes: p** Significance level obtained with the ANOVA test, $p < 0.05$. *$p < 0.05$: Compared to Group C. &$p < 0.05$: Compared to Group D. +$p < 0.05$: Compared to Group IR.
Abbreviation: n, Number of rats.

Table 4 Antioxidant Enzyme Activities and Oxidant (TBARS) Levels (Mean ± SD) in Kidney Tissues

	Group C (n = 6)	Group D (n = 6)	Group IR (n = 6)	Group D-IR (n = 6)	P**
TBARS (nmol/mg protein)	11.29 ± 1.02	12.60 ± 3.14	22.95 ± 1.69*,&	13.17 ± 3.32+	< 0.0001
AES (IU/mg protein)	0.55 ± 0.17	0.58 ± 0.25	1.53 ± 0.25*,&	0.72 ± 0.24 +	< 0.0001
GST (IU/mg protein)	1.39 ± 0.27	1.34 ± 0.29	1.27 ± 0.18	1.38 ± 0.16	0.810
CAT (IU/mg protein)	19.63 ± 3.77	15.53 ± 7.84	72.95 ± 21.48*,&	26.05 ± 5.76+	< 0.0001

Notes: p** Significance level obtained with the ANOVA test, $p < 0.05$. *$p < 0.05$: Compared to Group C. &$p < 0.05$: Compared to Group D. +$p < 0.05$: Compared to Goup IR.
Abbreviation: n, Number of rats.

Table 5 Serum AST, ALT, GGT, BUN, Creatinine Levels (Mean ± SD)

	Group C (n = 6)	Group D (n = 6)	Group IR (n = 6)	Group D-IR (n = 6)	p**
AST (U/L)	138.33 ± 15.86	167.17 ± 28.24	1350.66 ± 272.30*,&	917.50 ± 181.51*,&,+	< 0.0001
ALT (U/L)	68.83 ± 9.41	63.33 ± 14.36	276.67 ± 55.54*,&	163.00 ± 70.70*,&, +	< 0.0001
GGT (U/L)	7.33 ± 2.25	7.83 ± 1.60	11.17 ± 2.14*,&	8.83 ± 1.17+	0.009
Creatinine (mg/dL)	0.32 ± 0.03	0.43 ± 0.15	0.50 ± 0.17	0.45 ± 0.13	0.185
BUN (mg/dL)	28.83 ± 6.14	34.00 ± 16.66	44.83 ± 28.05	37.50 ± 9.73	0.457

Notes: p** Significance level obtained with the ANOVA test, $p < 0.05$. *$p < 0.05$: Compared to Group C. &$p < 0.05$: Compared to Group D. +$p < 0.05$: Compared to Group IR.
Abbreviation: n, Number of rats.

Serum ALT activity also significantly differed between the groups ($p < 0.0001$). ALT activity was higher in the IR group than in the C and D groups ($p<0.0001$ and $p=0.002$, respectively). Similarly, the D-IR group exhibited higher ALT activity than the C and D groups ($p < 0.0001$ and $p = 0.001$, respectively). In contrast, the D-IR group displayed lower ALT activity levels than the IR group ($p < 0.0001$) (Table 5).

Significant differences were observed between the serum GGT activity levels of the groups ($p = 0.009$). GGT activity was higher in the IR group than in the C and D groups ($p = 0.002$ and $p = 0.005$, respectively). Moreover, the D-IR group exhibited lower GGT activity than the IR group ($p = 0.040$) (Table 5).

No significant differences were observed between the groups' serum BUN and creatinine levels ($p = 0.457$ and $p = 0.185$, respectively) (Table 5).

Discussion

Although IR has been extensively explored across various organs and anti-inflammatory treatments, pancreatic IR remains relatively unexplored in the literature. Furthermore, previous experiments on pancreatic IR have predominantly focused on direct damage to the pancreas. Broader impacts on critical organ systems such as the kidneys and liver, which can influence postoperative outcomes, have received limited attention. In this study, we established an animal model of pancreatic IR and investigated the effects of dexmedetomidine pretreatment on kidney and liver injuries. To our knowledge, this study resulted in the first demonstration of dexmedetomidine's protective effects against the progression of kidney and liver injuries induced by pancreatic IR. Our observations are supported by biochemical and histological evidence.

The pancreas lacks the end arteries found in established ex vivo perfused organs, making it a low-flow organ. High perfusion pressure causes damage to and swelling of the pancreas, whereas low pressure may not provide sufficient perfusion.[30] Thus, the pancreas is vulnerable to swelling and damage due to ischemia-reperfusion events during surgeries such as pancreaticoduodenectomy, duodenum-preserving pancreatic head resection, distal pancreatectomy, and transplantation.[30,31]

Stress-induced damage to the pancreas also contributes to remote organ injury, particularly after surgery. Such damage may arise from compromised capillary perfusion after ischemia and diverted organ blood flow. IR triggers inflammatory pathways, generates reactive oxygen species, and activates vasoactive compounds, which collectively lead to endothelial cell damage and increased vascular resistance.[32,33] This triad, perfusion pressure, and vascular resistance can activate inflammatory pathways and thereby result in the impaired functioning of both the pancreas and remote organ systems.[34] The findings of this study demonstrated that pancreatic IR leads to significant histopathological changes in the liver and kidneys, even after a short period of circulatory disruption. This underscores the significance of maintaining vigilance during pancreatic surgeries or in any scenario involving the potential impairment of pancreatic perfusion. Notably, even in the absence of fully compromised laboratory values, subtle histopathological changes may indicate the initial phases of renal and hepatic compromise and exacerbate patients' clinical conditions. We propose that pretreatment with dexmedetomidine can mitigate this sequence of events.

Dexmedetomidine is frequently used for sedation in critical care settings and provides cardiovascular stability during surgery.[11,35] It has a short half-life and exhibits rapid tissue distribution, with few adverse effects.[36] In recent years, experimental investigations have corroborated the protective effects of dexmedetomidine on various organ systems, including the nervous,[12] cardiovascular,[16] respiratory,[14] renal,[13,37] hepatic,[37,38] and gastrointestinal[17] systems. It mitigates the inflammatory reaction, triggers antiapoptotic signaling pathways that protect cells from injury, regulates the release of catecholamines, eliminates excessive free radicals, reduces malondialdehyde, and enhances superoxide dismutase activity.[39]

TBARS, AES, GST, and CAT levels serve as indicators of oxidative stress.[28] In the present study, the hepatic and kidney tissues of rats subjected to dexmedetomidine before pancreatic IR injury exhibited significant reductions in their TBARS, AES, and CAT levels compared to those in the IR group. However, there were no differences between the GST levels of the groups. GST is primarily concentrated in the liver and undergoes swift release in response to injury. This release is followed by its rapid return to baseline levels, and the extent of this change is directly proportional to the severity of the injury.[40] Therefore, we attributed the absence of changes in GST levels to this specific response pattern.

In the course of acute pancreatitis, inflammatory cytokines such as IL-1b, IL-6, and tumor necrosis factor a (TNFa) are predominantly synthesized and released from the pancreas and subsequently into distant organs. In severe cases of acute pancreatitis, this process can cause systemic inflammatory response syndrome and multiple organ dysfunction.[41–43] Dexmedetomidine has demonstrated the capacity to mitigate the systemic inflammatory response and ameliorate local pancreatic damage in cases of severe acute pancreatitis by stimulating central α2-AR and reducing IL-1β, IL-6, TNF-α, myeloperoxidase, HMGB1, and NLRP3 activation.[36]

Although previous studies have not explored the impacts of dexmedetomidine on pancreatic IR-induced renal and hepatic injuries, its direct effects on renal and hepatic ischemia have been established.[39,44–46] Huang et al's meta-analysis of eight clinical randomized controlled trials showed that dexmedetomidine has a protective effect against liver IR injury during hepatectomy.[44] Similarly, in animal experiments concerning hepatic IR injury, the intraperitoneal administration of dexmedetomidine (at doses of 10 or 100 μg/kg) 30 min prior to hepatic ischemia led to elevated levels of superoxide dismutase, catalase, and glutathione, thereby mitigating damage to liver tissue.[47] Its positive effects on renal IR injury have also been widely demonstrated. Specifically, it reduces the release of renal noradrenaline and the stress-induced elevation of circulating noradrenaline levels and effectively regulates glomerular filtration and renal blood flow.[39,48,49] Intraperitoneal administration of 100 μg/kg dexmedetomidine during renal ischemia has been demonstrated to significantly decrease the levels of blood urea nitrogen and creatinine while concurrently increasing superoxide dismutase activity.[46]

The present study had certain limitations. First, although the protective effects of dexmedetomidine on the kidney and liver were successfully demonstrated through histopathological examinations and antioxidant enzyme level assessments, the investigation did not extend to examining potential pancreatic damage. Second, relying on BUN and creatinine, which are commonly preferred for diagnosing renal failure, did not yield significant results indicative of acute kidney injury. However, serum creatinine and BUN served as functional markers that were responsive only to a substantial loss of renal function, highlighting the limitation of functional renal reserves (approximately 20–40% in healthy kidneys).[50] Notably, these markers exhibit changes only during the later stages of kidney injury, which limits their capacity for the early detection of acute kidney injury when interventions can still be effective. Thus, the findings of this study emphasize the necessity for complementary markers or alternative diagnostic approaches to enable the early recognition of acute kidney injury during stages amenable to intervention and reversal.

Despite being favored as a sedative in intensive care units, dexmedetomidine is not commonly chosen for major abdominal surgeries. However, in cases of pancreatic surgery where pancreatic IR is anticipated, considering dexmedetomidine as an adjunct to general anesthesia could be beneficial. Although our histopathological findings indicated that dexmedetomidine induced distant organ damage in pancreatic IR cases, the immune mechanisms underlying this effect need to be explored in future studies.

Conclusion

This study revealed that the preemptive administration of dexmedetomidine prior to pancreatic IR leads to protective effects on kidney and liver tissues, as evidenced by histopathological and biochemical assessments. These findings point

to the potential application of dexmedetomidine in preventing kidney and liver injuries, particularly during pancreatic surgeries and in other circumstances characterized by diminished pancreatic blood flow.

Disclosure

The authors report no conflicts of interest in this work.

References

1. Maglione M, Ploeg RJ, Friend PJ. Donor risk factors, retrieval technique, preservation and ischemia/reperfusion injury in pancreas transplantation. *Current Opin Organ Transpl*. 2013;18:83–88. doi:10.1097/MOT.0b013e32835c29ef
2. Prudhomme T, Mulvey JF, Young LAJ, et al. Ischemia-reperfusion injuries assessment during pancreas preservation. *Int J Mol Sci*. 2021;22. doi:10.3390/ijms22105172
3. Abelha FJ, Botelho M, Fernandes V, Barros H. Determinants of postoperative acute kidney injury. *Critical Care*. 2009;13:1–10. doi:10.1186/cc7894
4. Causey MW, Maykel JA, Hatch Q, Miller S, Steele SR. Identifying risk factors for renal failure and myocardial infarction following colorectal surgery. *J Surg Res*. 2011;170:32–37. doi:10.1016/j.jss.2011.03.027
5. Kheterpal S, Tremper KK, Englesbe MJ, et al. Predictors of postoperative acute renal failure after noncardiac surgery in patients with previously normal renal function. *J Am Soc Anesthesiologists*. 2007;107:892–902.
6. Neeff H, Mariaskin D, Spangenberg H-C, Hopt UT, Makowiec F. Perioperative mortality after non-hepatic general surgery in patients with liver cirrhosis: an analysis of 138 operations in the 2000s Using Child and MELD scores. *J Gastrointestinal Surg*. 2011;15:1–11. doi:10.1007/s11605-010-1366-9
7. Grochowiecki T, Gałązka Z, Madej K, et al. Surgical complications related to transplanted pancreas after simultaneous pancreas and kidney transplantation. In: Transplantation Proceedings Elsevier; 2014:2818–2821.
8. Rydenfelt K, Kjøsen G, Horneland R, et al. Local postoperative graft inflammation in pancreas transplant patients with early graft thrombosis. *Transplant Direct*. 2024;10:e1567. doi:10.1097/TXD.0000000000001567
9. Herrero-Martínez J, Lumbreras C, Manrique A, et al. Epidemiology, risk factors and impact on long-term pancreatic function of infection following pancreas-kidney transplantation. *Clin Microbiol Infect*. 2013;19:1132–1139. doi:10.1111/1469-0691.12165
10. Lee S. Dexmedetomidine: present and future directions. *Kja*. 2019;72:323–330.
11. Carollo DS, Nossaman BD, Ramadhyani U. Dexmedetomidine: a review of clinical applications. *Curr Opin Anesthesiol*. 2008;21:457–461. doi:10.1097/ACO.0b013e328305e3ef
12. Cheng M, Gao T, Xi F, et al. Dexmedetomidine ameliorates muscle wasting and attenuates the alteration of hypothalamic neuropeptides and inflammation in endotoxemic rats. *PLoS One*. 2017;12:e0174894. doi:10.1371/journal.pone.0174894
13. Liang H, Liu H-Z, Wang H-B, Zhong J-Y, Yang C-X, Zhang B. Dexmedetomidine protects against cisplatin-induced acute kidney injury in mice through regulating apoptosis and inflammation. *Inflammation Res*. 2017;66:399–411. doi:10.1007/s00011-017-1023-9
14. Liu Z, Wang Y, Wang Y, et al. Dexmedetomidine attenuates inflammatory reaction in the lung tissues of septic mice by activating cholinergic anti-inflammatory pathway. *Int Immunopharmacol*. 2016;35:210–216. doi:10.1016/j.intimp.2016.04.003
15. C-l T, Li J, Zhao B, Shi S, Shen H, Z-y X. Effects of dexmedetomidine combined with sodium creatine phosphate on inflammation, oxidative stress, and neurological function recovery in patients undergoing intracranial hematoma evacuation: study protocol for a multi-center, prospective randomized parallel-cohort controlled trial. *Asia Pacif J Clin Trials*. 2017;2:1.
16. Dong A, Zhang Y, Lu S, Yu W. Influence of dexmedetomidine on myocardial injury in patients with simultaneous pancreas-kidney transplantation. *Evid Based Complement Alternat Med*. 2022;2022:1–8. doi:10.1155/2022/7196449
17. Zhang X-Y, Liu Z-M, Wen S-H, et al. Dexmedetomidine administration before, but not after, ischemia attenuates intestinal injury induced by intestinal ischemia-reperfusion in rats. *J Am Soc Anesthesiologists*. 2012;116:1035–1046.
18. Huang D-Y, Li Q, Shi C-Y, Hou C-Q, Miao Y, Shen H-B. Dexmedetomidine attenuates inflammation and pancreatic injury in a rat model of experimental severe acute pancreatitis via cholinergic anti-inflammatory pathway. *Chinese Med J*. 2020;133:1073–1079. doi:10.1097/CM9.0000000000000766
19. Li Y, Pan Y, Gao L, et al. Dexmedetomidine attenuates pancreatic injury and inflammatory response in mice with pancreatitis by possible reduction of NLRP3 activation and up-regulation of NET expression. *Biochem Biophys Res Commun*. 2018;495:2439–2447. doi:10.1016/j.bbrc.2017.12.090
20. Şengel N, Köksal Z, Dursun AD, et al. Effects of dexmedetomidine administered through different routes on kidney tissue in rats with spinal cord ischaemia–reperfusion injury. *Drug Des Devel Ther*;2022. 2229–2239. doi:10.2147/DDDT.S361618
21. Dembinski A, Warzecha Z, Ceranowicz P, et al. Pancreatic damage and regeneration in the course of ischemia-reperfusion induced pancreatitis in rats. *J Physiol Pharmacol*. 2001;52:1.
22. Von Dobschuetz E, Schmidt R, Scholtes M, et al. Protective role of heme oxygenase-1 in pancreatic microcirculatory dysfunction after ischemia/reperfusion in rats. *Pancreas*. 2008;36:377–384. doi:10.1097/MPA.0b013e31815ceb0e
23. Van Ye TM, Roza AM, Pieper GM, Henderson J, Johnson CP, Adams MB. Inhibition of intestinal lipid peroxidation does not minimize morphologic damage. *J Surg Res*. 1993;55:553–558. doi:10.1006/jsre.1993.1183
24. Aebi H. Catalase. *Method Enzym Anal Elsev*. 1974;1974:673–684.
25. Habig WH, Pabst MJ, Jakoby WB. Glutathione S-transferases: the first enzymatic step in mercapturic acid formation. *J Biol Chem*. 1974;249:7130–7139. doi:10.1016/S0021-9258(19)42083-8
26. Lowry O, Rosebrough N, Farr AL, Randall R. Protein measurement with the Folin phenol reagent. *J Biol Chem*. 1951;193:265–275. doi:10.1016/S0021-9258(19)52451-6
27. Abdel-Wahhab M, Nada S, Arbid M. Ochratoxicosis: prevention of developmental toxicity by L-methionine in rats. *J Appl Toxicol*. 1999;19:7–12. doi:10.1002/(SICI)1099-1263(199901/02)19:1<7::AID-JAT529>3.0.CO;2-G
28. Gobut H, Erel S, Ozdemir C, et al. Effects of cerium oxide on liver tissue in liver ischemia-reperfusion injury in rats undergoing sevoflurane anesthesia. *Exp Ther Med*. 2023;25:1–8. doi:10.3892/etm.2023.11863

29. Bostan H, Kalkan Y, Tomak Y, et al. Reversal of rocuronium-induced neuromuscular block with sugammadex and resulting histopathological effects in rat kidneys. *Renal Failure*. 2011;33:1019–1024. doi:10.3109/0886022X.2011.618972
30. Basile D P, Yoder M C. Renal endothelial dysfunction in acute kidney ischemia reperfusion injury. *Cardiov Haematol Disord Drug Targ*. 2014;14:3–14. doi:10.2174/1871529X1401140724093505
31. Ho CK, Kleeff J, Friess H, Büchler MW. Complications of pancreatic surgery. *HPB*. 2005;7:99–108. doi:10.1080/13651820510028936
32. Benz S, Pfeffer F, Adam U, Schareck W, Hopt U. Impairment of pancreatic microcirculation in the early reperfusion period during simultaneous pancreas-kidney transplantation. *Transplant Int*. 1998;11:S433–S435. doi:10.1111/j.1432-2277.1998.tb01175.x
33. Muñoz-Casares FC, Padillo FJ, Briceño J, et al. Melatonin reduces apoptosis and necrosis induced by ischemia/reperfusion injury of the pancreas. *J Pineal Res*. 2006;40:195–203. doi:10.1111/j.1600-079X.2005.00291.x
34. Baertschiger RM, Berney T, Morel P. Organ preservation in pancreas and islet transplantation. *Current Opin Organ Transplant*. 2008;13:59–66. doi:10.1097/MOT.0b013e3282f44a63
35. Arcangeli A, D'alo C, Gaspari R. Dexmedetomidine use in general anaesthesia. *Curr Drug Targ*. 2009;10:687–695. doi:10.2174/138945009788982423
36. Chen R, Dou X-K, Dai M-S, Sun Y, Sun S-J, Wu Y. The role of dexmedetomidine in immune tissue and inflammatory diseases: a narrative review. *Eur Rev Med Pharmacol Sci*. 2022;26:1.
37. Arslan M. Effect of dexmedetomidine on ischemia-reperfusion injury of liver and kidney tissues in experimental diabetes and hepatic ischemia-reperfusion injury induced rats. *Anaesth Pain Intensive Care*. 2019;2019:1.
38. Wang Y, Wu S, Yu X, et al. Dexmedetomidine protects rat liver against ischemia-reperfusion injury partly by the α2A-adrenoceptor subtype and the mechanism is associated with the TLR4/NF-κB pathway. *Int J Mol Sci*. 2016;17:995. doi:10.3390/ijms17070995
39. Bao N, Tang B. Organ-protective effects and the underlying mechanism of dexmedetomidine. *Mediators Inflammation*. 2020;2020. doi:10.1155/2020/6136105
40. Smith GS, Walter GL, Walker RM. Clinical pathology in non-clinical toxicology testing. *Haschek and Rousseaux's Handbook of Toxicologic Pathology Elsevier*. 2013;2013:565–594.
41. Vasseur P, Devaure I, Sellier J, et al. High plasma levels of the pro-inflammatory cytokine IL-22 and the anti-inflammatory cytokines IL-10 and IL-1ra in acute pancreatitis. *Pancreatology*. 2014;14:465–469. doi:10.1016/j.pan.2014.08.005
42. Maduzia D, Ceranowicz P, Cieszkowski J, et al. Administration of warfarin accelerates the recovery in ischemia/reperfusion-induced acute pancreatitis. *J Physiol Pharmacol*. 2020;71:417–427.
43. Frossard J-L, Pastor CM. Experimental acute pancreatitis: new insights into the pathophysiology. *Front Biosci*. 2002;7:257.
44. Huang Y-Q, Wen R-T, X-T L, Zhang J, Yu Z-Y, Feng Y-F. The protective effect of dexmedetomidine against ischemia-reperfusion injury after hepatectomy: a meta-analysis of randomized controlled trials. *Front Pharmacol*. 2021;12:747911. doi:10.3389/fphar.2021.747911
45. Fayed NA, Sayed EI, Saleh SM, Ehsan NA, Elfert AY. Effect of dexmedetomidine on hepatic ischemia–reperfusion injury in the setting of adult living donor liver transplantation. *Clin Transplant*. 2016;30:470–482. doi:10.1111/ctr.12713
46. Cakir M, Polat A, Tekin S, et al. The effect of dexmedetomidine against oxidative and tubular damage induced by renal ischemia reperfusion in rats. *Renal Failure*. 2015;37:704–708. doi:10.3109/0886022X.2015.1011550
47. Şahin T, Begeç Z, Toprak Hİ, et al. The effects of dexmedetomidine on liver ischemia–reperfusion injury in rats. *J Surg Res*. 2013;183:385–390. doi:10.1016/j.jss.2012.11.034
48. Scheinin M, Kallio A, Koulu M, Viikari J, Scheinin H. Sedative and cardiovascular effects of medetomidine, a novel selective alpha 2-adrenoceptor agonist, in healthy volunteers. *Br J Clin Pharmacol*. 1987;24:443–451. doi:10.1111/j.1365-2125.1987.tb03196.x
49. Jaionen J, Hynynen M, Kuitunen A, et al. Dexmedetomidine as an anesthetic adjunct in coronary artery bypass grafting. *J Am Soc Anesthesiologists*. 1997;86:331–345.
50. van Duijl TT, Ruhaak LR, de Fijter JW, Cobbaert CM. Kidney injury biomarkers in an academic hospital setting: where are we now? *Clin Biochem Rev*. 2019;40:79–97.